

SUPPLEMENTAL MATERIALS

***Xenorhabdus nematophila* bacteria shift from mutualistic to virulent Lrp-dependent phenotypes within the receptacles of *Steinernema carpocapsae* insect-infective stage nematodes.**

Mengyi Cao^a and Heidi Goodrich-Blair Department of Bacteriology, University of Wisconsin-Madison, WI 53706, USA; Department of Microbiology, University of Tennessee-Knoxville, TN 37996

Table S1. Bacterial strains used in this research.

Strain or plasmids	Relevant genetic characteristic(s)	Source/references
HGB1059	<i>X. nematophila</i> HGB800 <i>lrp-2::kan</i>	(Cowles <i>et al.</i> , 2007)
HGB2261	HGB1059 <i>attTn7::P_{fliC}-gfp</i> / <i>P_{lac}-rfp</i>	(Cao <i>et al.</i> , 2017)
HGB2262	HGB2261 <i>kefA::pMYC4</i> (low Lrp); <i>attTn7::P_{fliC}-gfp</i> / <i>P_{lac}-rfp</i>	(Cao <i>et al.</i> , 2017)
HGB2263	HGB2261 <i>kefA::pMYC5</i> (high Lrp); <i>attTn7::P_{fliC}-gfp</i> / <i>P_{lac}-rfp</i>	(Cao <i>et al.</i> , 2017)
HGB2264	HGB1969, vector cured, <i>attTn7::P_{fliC}-gfp</i> / <i>P_{lac}-rfp</i>	This study
HGB1262	<i>E. coli</i> carrying plasmid pURR25-mini Tn7KR- <i>gfp</i>	(Teal <i>et al.</i> , 2006; Chaston <i>et al.</i> , 2013)
HGB2317	<i>X. nematophila lrp-2::kan attTn7::Tn7KR-gfp</i>	This study
HGB2318	<i>X. nematophila lrp-2::kan kefA::pMYC4</i> (low Lrp); <i>attTn7::Tn7KR-gfp</i>	This study
HGB2319	<i>X. nematophila lrp-2::kan kefA::pMYC5</i> (high Lrp); <i>attTn7::Tn7KR-gfp</i>	This study
HGB1783	<i>E. coli</i> S17- λ pir carrying plasmid pJMC001	(Chaston <i>et al.</i> , 2013)
HGB2108	<i>X. nematophila lrp-2::kan, kefA::P_{lac}-gfp</i> ; plus pEH54 (low Lrp plasmid)	This study
HGB2109	<i>X. nematophila lrp-2::kan, kefA::P_{lac}-gfp</i> ; plus pEH56 (high Lrp plasmid)	This study
HGB2190	<i>X. nematophila lrp-2::kan, kefA::P_{lac}-gfp</i> ; plus pKV69 (vector plasmid)	This study
HGB1969	<i>X. nematophila</i> wild type virulent strain plus pKV69 (vector plasmid)	(Hussa <i>et al.</i> , 2015)
HGB1970	<i>X. nematophila</i> wild type virulence-attenuated strain plus pKV69 (vector plasmid)	(Hussa <i>et al.</i> , 2015)
HGB2110	HGB1969, vector cured, <i>attTn7::Tn7KR-gfp</i>	This study
Plasmids		
pURR25-mini Tn7/KR-GFP	Tn7 transposon plasmid with <i>P_{lac}-gfp</i> , Cm ^R , Kan ^R	(Teal <i>et al.</i> , 2006; Chaston <i>et al.</i> , 2013)
pJMC1	Plasmid carries <i>P_{lac}-gfp</i> that integrates at <i>kefA</i> , Cm ^R	(Chaston <i>et al.</i> , 2013)
pKV69	Multicopy mobilizable vector; Cm ^R , Tet ^R	(Visick and Skoufos, 2001)
pEH54	pKV69 with <i>lrp</i> in opposite orientation relative to <i>P_{lac}</i>	(Hussa <i>et al.</i> , 2015)
pEH56	pKV69 with <i>lrp</i> under control of <i>P_{lac}</i>	(Hussa <i>et al.</i> , 2015)
pMYC1	<i>P_{fliC}-gfp</i> / <i>P_{lac}-rfp</i> reporter at <i>attTn7</i> , Erm ^R , Kan ^R	(Cao <i>et al.</i> , 2017)

Figure S1: Overview of experimental assessments of physiological aspects in symbiotic life cycle. The tan circle represents an agar plate with a *X. nematophila* lawn of wild type or high-, low-, or no-Lrp bacteria as described in the main text, on which aposymbiotic (symbiont-free) *S. carpocapsae* nematode IJs are seeded. These nematodes develop on the *X. nematophila* lawns into first generation fourth stage juveniles (J4) and adult males and females that mate and produce eggs that either continue to develop through this reproductive phase of the life cycle: J1-J4 and adults, or that develop through the transmission phase of the life cycle: pre-IJs, immature IJs, mature IJs that emerge over time (as indicated by the emergence time ET), and IJ that age over time post-emergence. Each developmental stage or phenotype tested in the current paper or in Cao *et al.*, 2017 is indicated according to the figure in which the data are presented. When used, blue and red font indicate that high or low Lrp, respectively, is optimal for that phenotype, and this is indicated generally by the brackets and labels shown at the top of the figure. Note that a high-Lrp state is optimal for colonization through reproductive stages and during development of the transmission stage nematode, but that the low-Lrp state allows higher bacterial loads (CFU/IJ) in late-emerging IJs and occurs in increasing frequency as emerged IJs age.

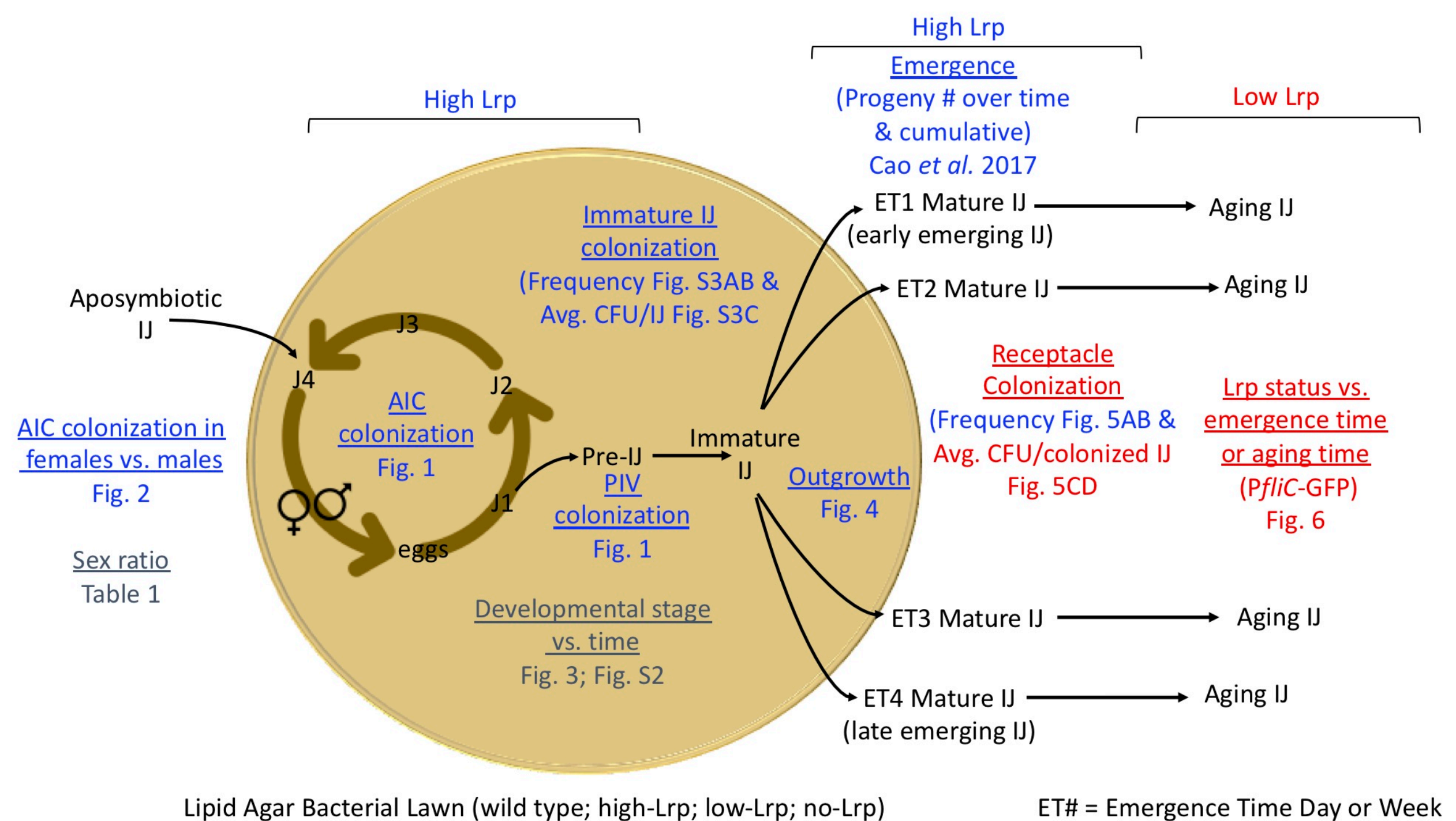


Figure S2: *S. carpocapsae* nematode developmental stages over time on bacterial lawns.

A second independent experiment (in addition to the experiment shown in Fig. 3) was conducted to observe nematode development on *X. nematophila* bacterial lawns expressing high-*lrp*, low-*lrp*, and no-*lrp*. Aposymbiotic IJs were seeded onto lawns and observed over time. Shown are the percentages on each lawn of observed adults (red), juveniles (including open-intestine pre-IJs; blue), constricted pre-IJs (green), and IJs (white) at days 6 (A), 8 (B), 10 (C), 12 (D), 14 (E), 17 (F), 21 (G) post seeding of aposymbiotic IJs on bacterial lawns. Percent total nematode colonization (H) includes colonized nematodes in all developmental stages (adults, juveniles, pre-IJs, and IJs). Percent population (A-G) and percent colonization (H) are shown as the average and standard error of five biological replicates each from a different batch of conventional IJs seeded onto plates to initiate the experiment. Each biological replicate represents one individual plate. Statistical analysis was performed within each life-stage across time points using One-way ANOVA followed by Tukey's multiple comparison. Significant differences ($P \leq 0.05$, *, $P \leq 0.01$, **, $P \leq 0.001$, ***) between treatments within each life stage are shown with brackets below for panel B (blue bars) and panel C (blue bars). The rest of the comparisons are shown with brackets above the compared treatments. Total number of nematodes screened: 4110 (on high-*lrp* bacteria); 4056 (on low-*lrp* bacteria), 4008 (on no-*lrp* bacteria).

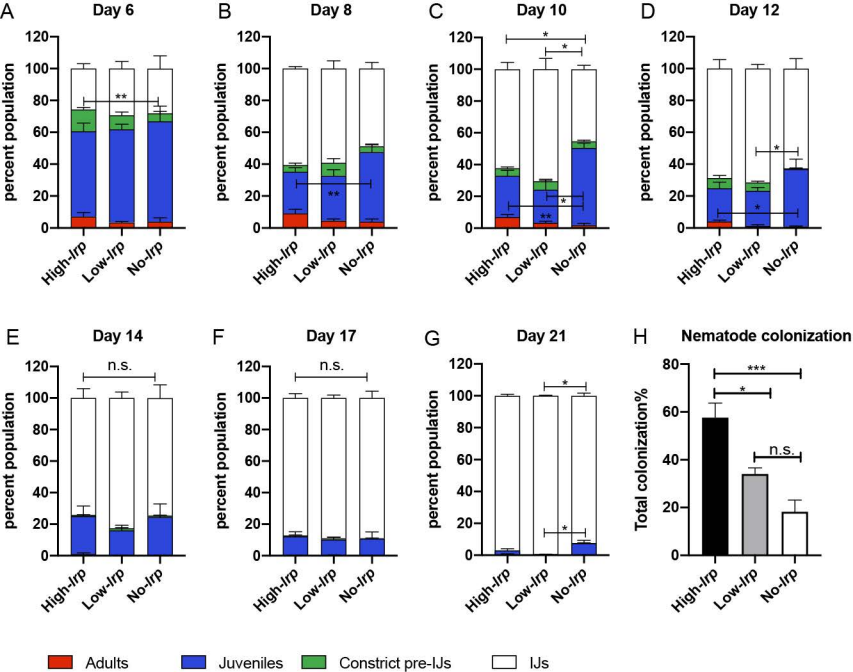
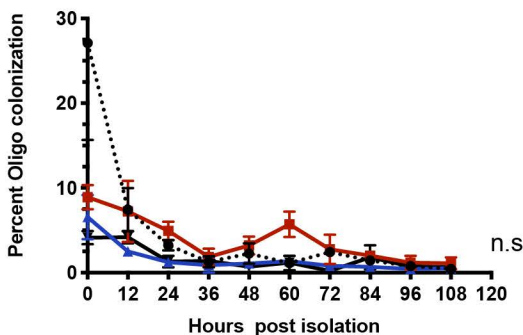
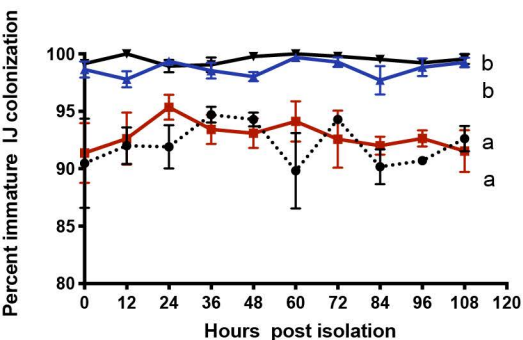


Figure S3: Oligo-colonization frequency (A), total colonization frequency (B), and average CFU per colonized nematode (C) in immature IJs developed on lawns of *X. nematophila* expressing high-*lrp*, low-*lrp*, no-*lrp* from the bacterial genome. Immature IJs were isolated from bacterial lawns and maintained in water and sampled every 12 hours over 120 hours post isolation. At each time point of sampling, oligo-colonization (a few individual bacterial cells in the IJ receptacle) frequency (A), colonization (including oligo and non-oligo colonization) frequency (B) were assessed by fluorescence microscopy. To assess average CFU per colonized immature IJ at each time point (C), approximately 100 nematodes were surface-sterilized and grounded. Bacteria from the IJ receptacle were recovered on the LB agar plate to approximate CFU in the population. CFU per colonized IJ were assessed using the total number of CFU in the grounded nematode population divided by number of colonized IJs calculated by colonization frequency. Average of three biological replicates (three batches of conventional nematodes) and standard errors are shown. Statistical analysis were performed by Two-way ANOVA test followed by Tukey's multiple comparison and different letters indicate significant differences ($P \leq 0.05$)

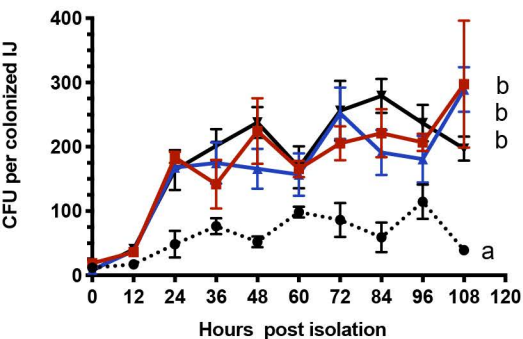
A. Oligo colonization in the immature IJs



B. Colonization in the immature IJs



C. Average CFU per colonized immature IJ



- *lrp::kan; Tn7::Plac-gfp*
- *kefA::low-lrp; Tn7::Plac-gfp*
- ▲ *kefA::high-lrp; Tn7::Plac-gfp*
- ▼ wild type; *Tn7::Plac-gfp*